

# The effects of central-region conditions on time structure and quality of cyclotron beams

M. Reiser  
*University of Maryland, U. S. A.*

## ABSTRACT

Time structure, emittance, particle intensity and energy spread of a cyclotron beam are largely determined by central region conditions and can be defined through choice of orbit geometry and use of defining slits. The fundamental limit of beam equality is given by the intrinsic emittance and phase-space density which the beam would have under d.c. conditions. In the actual case of rf acceleration, ion intensity and energy gain become a function of phase with respect to the rf voltage and the effective emittance increases due to radial dispersion in the magnetic field. For a fixed energy spread at extraction and hence a given spread of orbit centres, the phase width or microscopic duty factor of the beam, is the larger the smaller the orbit geometry at injection, i.e. the lower the dee voltage. On the other hand, space-charge effects, short-pulse requirements for time-of-flight experiments, etc., favour high dee voltage and hence a large orbit geometry. The Maryland cyclotron was designed to provide some flexibility between the two extremes, permitting a variation of orbit geometry between 155 turns (single-turn extraction) and 700 turns (multiturn extraction).

## 1. INTRODUCTION

It is well known that the pertinent characteristics of a cyclotron beam—time structure, radial and axial emittance, particle intensity and energy spread—are to a large degree determined by conditions in the central region. More than a decade of intensive studies and improvements of field mapping and computer techniques have led to an increasingly better understanding of the initial acceleration process. The review paper at the last cyclotron conference by H. Blosser<sup>1</sup> summarised some of the major achievements in central-region design and the resulting improvements in actual cyclotron performance. The relatively large

number of invited and contributed papers on beam quality at the present conference are an impressive testimony of the progress that was made in the central-region problems which for a long time had been the least understood aspect of cyclotron performance. Indeed, we have reached the point where initial orbits—as well as the subsequent ion motion through the cyclotron—can be calculated with a previously unexpected degree of accuracy such that measured beam patterns and theory are in excellent agreement.

The present paper will review and discuss the major factors that determine the time structure and beam quality during the initial acceleration process. Much of it is based on the author's central-region studies for the Karlsruhe, Michigan State, and NRDL cyclotrons as well as the results of recent work at the University of Maryland. Relevant features of the design philosophy adopted for the Maryland cyclotron will be discussed and serve to illustrate the various physics aspects of central-region beam dynamics.

Ion source and beam emittance, median-plane motion, vertical focusing, and space-charge effects are the major topics of the following review. The main emphasis is on orbit geometry which, as will be shown, determines to a significant degree the time structure of the acceptable ion beam. In the Maryland cyclotron, enough flexibility was provided to vary the orbit geometry—within certain limits—and thus give the experimenter the option of either large or narrow phase width. Details of the Maryland cyclotron and central-region design not discussed here can be found in other publications.<sup>2, 3</sup>

## 2. INTRINSIC EMITTANCE AND CYCLOTRON BEAM OPTICS

### 2.1. *Ion source and static beam emittance*

Practically all isochronous cyclotrons are now using the chimney-type ion source first developed at Oak Ridge by Livingston and Jones. Design details may vary somewhat depending on the peculiarities of a given machine. Thus, at some places the 'chimney' is made of carbon, while at others copper is used with watercooling and tantalum or molybdenum inserts containing the output slit. Our chimney at Maryland is made entirely of tantalum. The ion source is inserted axially and moves in one of two radial slots which are 180° apart and therefore produce a small second harmonic with negligible effect on the beam dynamics.

Ion sources of the Oak Ridge type are capable of producing maximum proton currents (under d.c. conditions) between 10 mA and several hundred milliamperes depending on the size of the output slit, the extraction voltage and the arc conditions. The radial and axial emittance of a cyclotron ion source was measured for the first time by Mallory<sup>4</sup> at Michigan State University in an ion-source testing facility (which has since been transferred to the University of Maryland). For an output-slit size of 1.5 mm × 9.5 mm, which is typical for most cyclotrons, a proton beam of 5 mA, and a d.c. extraction voltage of 30 kV the radial as well as the axial emittance was found to be in the neighbourhood of 200 mm mrad. The actual value depended on arc conditions and chimney geometry. A recessed output slit with face angle of 20° improved the emittance and provided good initial focusing of the beam in agreement with a previous theoretical study by the author.<sup>5</sup> Mallory deduced from his measurements that the luminosity increased with arc (and output beam) current; typical values were 15 A/cm<sup>2</sup>-sterad for an arc current of 1 A and 40 A/cm<sup>2</sup>-sterad for 5 A. He did not investigate how emittance and output current depend on the extraction

voltage  $V_o$  and the source-puller spacing  $d$ . From other ion source studies we know, however, that the output current shows roughly the  $V_o^{3/2}$  dependence predicted by Child's Law (under space charge conditions) and then saturates as the voltage exceeds a certain value which is typically in the range of 20 to 40 kV.

## 2.2. Linear optics and intrinsic beam width

For the discussion to follow let us now assume an ion source, with the characteristics described above, injecting a beam into the cyclotron. If the entire acceleration process in the cyclotron would be accomplished by static electric fields in the gaps we would have a well-defined spiralling beam path with separated orbits until the decreasing radial separation of the orbits due to the energy gain equals the intrinsic radial width of the beam. The initial orbits would look similar to those shown in Fig. 1. This picture illustrates the orbit pattern (with intrinsic betatron amplitudes) of a group of ions all starting at the *same* time from the ion source, as calculated for the Maryland cyclotron. Assuming that linear optics prevails throughout the cyclotron, the intrinsic radial width

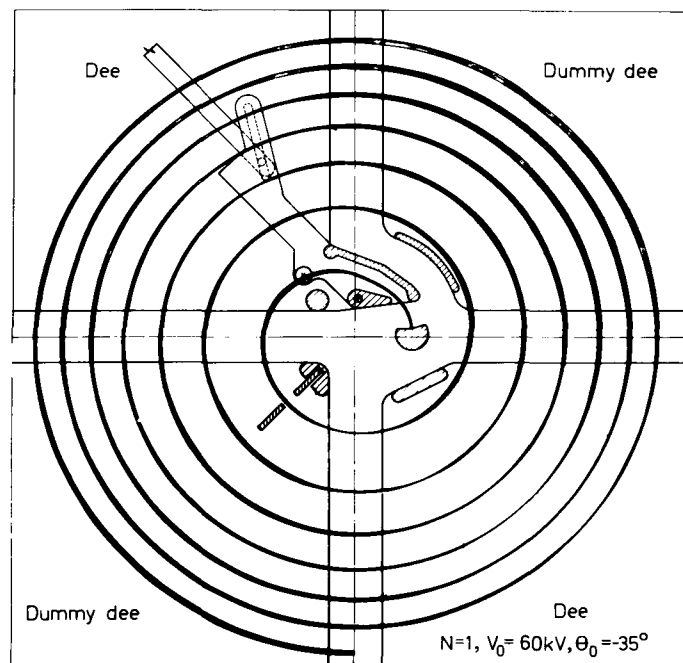


Fig. 1. Initial orbits with intrinsic radial amplitudes for protons ( $\theta_0 = -35^\circ$ ,  $V_0 = 60$  kV) in  $N = 1$  mode of Maryland cyclotron

would have an average value given by the source slit (1.5 mm, for example). The peak amplitude,  $\xi_m$ , of the associated betatron oscillations is proportional to the initial orbit radius,  $R_1$ , according to the relation  $\xi_m = \alpha_o R_1 / \nu_r$ , where  $\alpha_o$  is the initial divergence angle. Taking  $\nu_r = 1$  and a half angle of  $\alpha_o = 50$  mrad (consistent with an emittance of 200 mm mrad) the intrinsic maximum beam width,  $2\xi_m$ , would vary between approximately 2 mm (for  $R_1 = 2$  cm) and 4 mm

(for  $R_1 = 4$  cm) in most existing cyclotrons. Likewise the average vertical beam height is given by the source slit height (10 mm, for example). However, the maximum amplitude varies more than is the case in the radial motion due to electric focusing and the radial dependence of the magnetic betatron frequency,  $\nu_z$ , in the centre. Adiabatic damping reduces the amplitudes; however, this effect is negligible at energies below 100 MeV. Beam passage through resonances or nonlinear field regions, on the other hand, leads to—usually irreversible—distortions of the phase-space area. To avoid such phase-space deterioration in the vertical motion, for example, the beam should always remain within the linear region of the electric and magnetic fields close to the median plane. Field maps and orbit calculations suggest that this linear region is approximately 30% of the smallest gap height. In most cyclotrons the tolerable vertical beam amplitude is limited by the electric field in the centre and thus the internal dee height near the ion source. In cyclotrons with small magnet gaps and dees in the valleys the magnetic field may also shrink the useful region for undistorted vertical beam transmission. What this says is that any reduction of dee height and/or magnet gap requires a proportional reduction of vertical beam height and ion source slit and may, therefore, not necessarily increase the usable beam intensity despite an improvement of vertical focusing. (It appears that this argument has generally been overlooked by cyclotron designers in the discussions of small-gap vs large-gap machines.) This point will be discussed a little further in the chapter on space-charge effects.

Neglecting now any couplings between radial and vertical motion, beam losses due to non-linearities, or the effect of defining slits, the (intrinsic) emittance,  $A_2$ , of our idealised cyclotron beam at full energy,  $E_2$ , is determined by the source emittance,  $A_1$ , at injection energy,  $E_1$ , according to the relation

$$A_2 = A_1 (E_1/E_2)^{1/2} \quad (1)$$

Thus, for  $A_1 = 200$  mm mrad,  $E_1 = 30$  keV, as measured by Mallory, one would expect an intrinsic emittance of  $A_2 \approx 5$  mm mrad for a 50 MeV cyclotron, and roughly 3 mm mrad for a 150 MeV machine.

### 2.3. Beam emittance in the case of rf acceleration

When the time-varying field of the cyclotron rf system rather than a d.c. field is used to extract the ions from the source three effects occur. (1) The extracted ion intensity, or phase-space density, becomes a function of time. (2) An energy spread is introduced as particles crossing the source-puller gap at different phases gain a different amount of energy. (3) The emittance of the beam increases as a result of the spatial dispersion due to the magnetic field.

As no phase-space density measurements have yet been made for this condition (they are exceedingly difficult to do), we can only apply general arguments, in combination with results of calculations, to discuss these effects and their implication for cyclotron design and beam characteristics. Thus we know from single-particle dynamics that, due to the finite transit time, the peak energy gain occurs at an earlier phase than the peak rf voltage. Furthermore, the radial dispersion (due to different starting phase) has a minimum for the group of particles starting near the phase of maximum energy gain. This is illustrated in Fig. 2, which shows the calculated energy gain and transit time in the source-puller gap for protons in the Maryland cyclotron at dee voltages of 60 and

90 kV. In the 60 kV case the phase of maximum energy gain is  $-30^\circ$  as compared to  $0^\circ$  for a narrow gap with negligible transit time. It has been shown in a previous paper<sup>6</sup> that energy gain and transit time are determined by the scaling parameter

$$\chi = \frac{d^2 B^2 q/m}{V_0} \quad (2)$$

where  $d$  is the gap width,  $V_0$  the dee voltage,  $B$  the magnetic field, and  $q/m$  the specific charge of the particles. For increasing values of  $\chi$  the peak-energy phase shifts towards the  $-90^\circ$  phase; it remains constant in a cyclotron with constant orbit geometry ( $B^2/V_0 = \text{const}$ ) provided the source-puller gap remains fixed. Space-charge will tend to increase the transit time, as we know from the static case, and probably also effect the peak energy gain as well as the phase at which it occurs. However, this problem has not yet been assessed quantitatively due to the difficulty of a theoretical treatment. The question where in the rf phase interval the peak beam intensity occurs is also coupled with the unknown space-charge problem. We can only argue qualitatively that there exist two situations. (1) The peak dee voltage,  $V_0$ , exceeds the saturation limit,  $V_s$ , in which case the intensity-versus-phase curve should exhibit a flat top over the phase interval  $\Delta\theta$  where the instantaneous voltage  $V_0 \cos \theta \geq V_s$  (say about 30 kV). (2) Under pure space-charge conditions one would expect an intensity peak which occurs at a negative phase<sup>6</sup> close to the peak-energy phase approaching the  $(V_0 \cos \theta)^{3/2}$  dependence in the quasi-static case (where the transit time is negligibly small compared to the rf period).

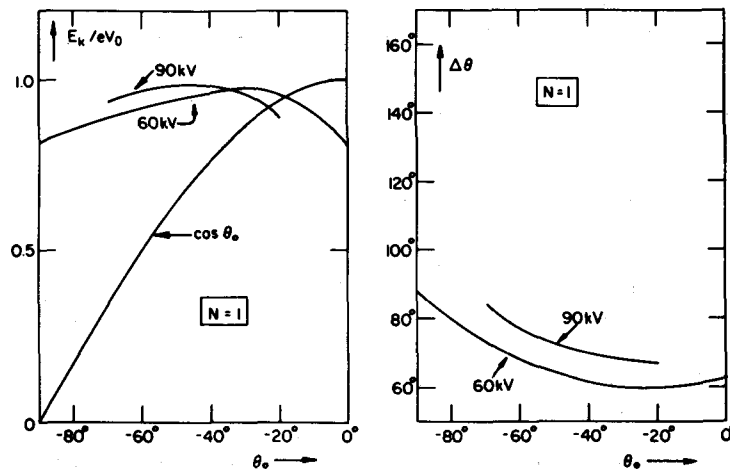


Fig. 2. Relative energy gain and transit phase angle in source-puller gap vs starting phase  $\theta_0$  for  $V_0$  of 60 and 90 kV in  $N = 1$  mode

### 3. CENTRAL ORBIT GEOMETRY AND DUTY FACTOR

#### 3.1. Spread of centre points due to rf acceleration

The radial motion of ions through the cyclotron is commonly described in terms of the equilibrium orbit,  $\rho_o(\Phi)$ , and the displacement  $\xi(\Phi) = r - \rho_o$ ,  $\xi' = d\xi/d\Phi$  (or  $\Delta p_r = m\omega \xi'$ ) of a given particle from the equilibrium orbit. After the first few revolutions coupling between radial and azimuthal motion becomes negligibly small, and by Liouville's Theorem the area occupied by the beam in  $r - p_r$  or, if  $m\omega$  does not change, in  $\xi - \xi'$  space remains constant. An equivalent description, which is better suited to discuss the effects of rf phase on ion motion, is the instantaneous centre point,  $r_c, \Phi_c$ , of a particle. If the flutter is neglected, i.e. if we consider only the average field,  $\bar{B}(r)$ , then the equilibrium orbit is a circle with radius  $\rho_o$ , and the local radius of curvature,  $\rho$ , of a particle displaced from the equilibrium orbit is by definition:

$$\rho = \frac{mv}{q \bar{B}(r)} = \frac{p}{q \bar{B}(\rho_o)} \frac{1}{1 + \bar{k} \xi/\rho_o} \quad (3)$$

where

$$\bar{k} = \frac{r}{\bar{B}} \frac{d\bar{B}}{dr}.$$

It can be shown that the co-ordinates of the instantaneous centre points are related to the displacement  $\xi, \xi'$  by the equations:

$$r_c^2 = (1 + \bar{k})^2 \xi^2 + \xi'^2 = \nu_r^4 \xi^2 + \xi'^2 \quad (4)$$

$$\sin(\Phi_c - \Phi) = \frac{\xi'}{r_c} \quad (5)$$

If  $\xi_m(\Phi_m)$  denotes the maximum displacement from the equilibrium orbit, then we can also write:

$$r_c \approx \nu_r \xi_m \left[ 1 + \frac{\nu_r^2 - 1}{2} \cos \nu_r (\Phi - \Phi_m) \right]. \quad (6)$$

The instantaneous centre point,  $r_c$ , thus describes a path with average radial co-ordinate of  $\nu_r \xi_m$  and a small periodic amplitude variation as the particle performs its betatron oscillation about the equilibrium orbit.

A particle can therefore be described either by a point in  $r - p_r$  phase space or by its instantaneous centre point in  $r - \Phi$  space. Likewise, the entire beam may be represented by a distribution of points filling a certain area in phase space or by the distribution of centre points occupying an equivalent area in  $r - \Phi$  space (this is also discussed in a paper by Lawson).<sup>7</sup> Both areas remain essentially constant after the coupling effects during the initial motion have disappeared.

To discuss the effects of rf phase on ion motion we shall now neglect the intrinsic radial emittance, i.e. we consider the ion source as a point source from which the particles emerge with zero initial velocity. First, consider the idealised situation with uniform  $B$  field, illustrated in Fig. 3, where the ions are injected into a  $180^\circ$  dee and the gap width is so small that the transit time is zero. Ions

leaving the source at different rf phase,  $\theta_o$ , gain an energy of  $q V_o \cos \theta_o$  resulting in different radii and centre points (1 to 5 in the figure). At the next gap crossing the radius increases and the group of centre points is shifted as shown in the figure (1' to 5'). If the source slit is at  $y = 0, x = x_o$ , the initial centre-point co-ordinate is  $\Phi_c = \pi$  and

$$r_c = x_o - \rho = x_o - R_o (\cos \theta_o)^{1/2} \quad (7)$$

where

$$R_o = \frac{1}{B} (2V_o m_o/q)^{1/2}.$$

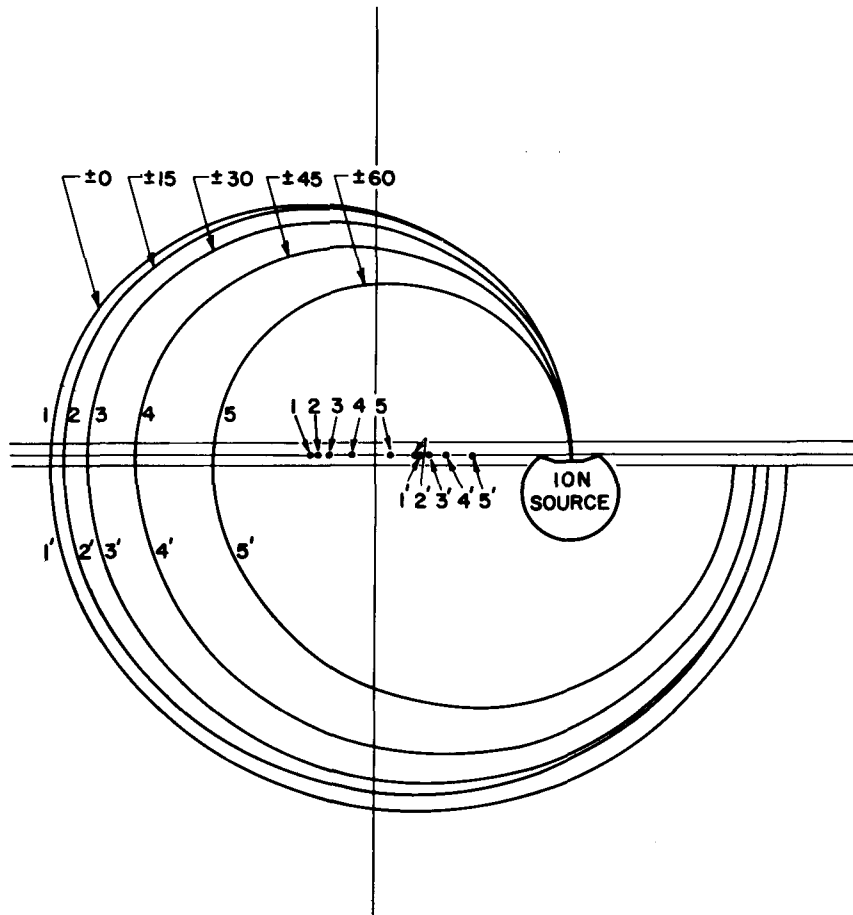


Fig. 3. First orbits and centre points in idealised case (narrow gap, uniform B field)

The initial centre spread  $\Delta r_c$  associated with particles leaving the source in the phase interval  $\Delta \theta_o = 2\theta_o$  is:

$$\Delta r_c = R_o [1 - (\cos \theta_o)^{1/2}] = \frac{1}{B} (2V_o m_o/q)^{1/2} [1 - (\cos \theta_o)^{1/2}]. \quad (8)$$

The centre spread for a given group of particles with phase width  $\Delta\theta_o$  is thus seen to be proportional to  $R_o$ , which represents a scale factor for the orbit geometry, or, for given  $B$  field, to  $V_o^{1/2}$ . The larger  $R_o$  (or  $V_o$ ) the smaller is the phase width of the beam that can be packed into a given  $\Delta r_c$ .

If we consider the other extreme of a large gap  $d$  where the first orbit is entirely within the electric field, we find<sup>8</sup>—assuming a uniform electric and magnetic field—that:

$$\Delta r_c = \frac{d}{\chi} \sin \theta_o = \frac{R_o^2}{2d} \sin \theta_o = \frac{m_o V_o}{qB^2 d} \sin \theta_o. \quad (9)$$

In this case the initial centre spread for a beam of phase width  $\Delta\theta = 2\theta_o$  is found to be proportional to  $R_o^2$  (or  $V_o$ ).

Actual cyclotrons have a central geometry somewhere in between the two extreme situations of narrow and wide gap, which implies that the spread of centre points for a group of ions with given phase width  $\Delta\theta_o$  is proportional to  $R_o^\alpha$ , where  $1 < \alpha < 2$ .

The relative energy spread  $\Delta E/E_f$  of the accelerated beam at full radius,  $r_f$ , is determined by the centre spread according to (non-relativistic case):

$$\frac{\Delta E}{E_f} = 2 \frac{\Delta r_c}{r_f}. \quad (10)$$

The desired energy resolution in a given cyclotron thus fixes  $\Delta r_c$  and hence the phase width  $\Delta\theta_o$  of the beam. It follows from the above discussion that the duty factor ( $\Delta\theta_o/2\pi$ ) of the accelerated beam with fixed  $\Delta E/E_f$  is the larger the smaller the orbit geometry or the dee voltage. The ideal cyclotron for large duty factor is therefore a machine with a large number of turns and—by implication—multiturn extraction. In fact, ideally one would want the centre spread to be comparable to the intrinsic radial width of the beam.

To check the validity of these analytical considerations we computed the central orbits of protons for a given electric and magnetic field geometry in the Maryland cyclotron (electric data was obtained from the electrolytic-tank, magnetic field from full-scale magnet measurements). For a dee voltage of  $V_o = 60$  kV the centre points (after several turns) of particles leaving the source between  $-90^\circ$  and  $0^\circ$  form the distribution plotted in Fig. 4(a). We then reduced the dee voltage by a factor of 2, to 30 kV, and the geometry accordingly by a factor of  $\sqrt{2}$ . The area filled by the centre points (for the same group of ions) was then found to be smaller by roughly a factor of 2 as seen in Fig. 4(b). These results indicate that in our special case the centre spread follows the  $R_o^2$  dependence of an ideal large-gap cyclotron.

It is clear, of course, that most other cyclotron-design considerations are in favour of a large dee voltage and a small number of turns (e.g. space requirements for the ion source and puller, space-charge effects, magnetic field error, resonance traversal, etc.). In practice one must therefore try to achieve a reasonable balance between the diverging requirements. Ideally one would like to have both a beam with large duty factor, hence small dee voltage with multiturn extraction system, and a narrow phase width (for time-of-flight work) requiring large dee voltage and single-turn extraction. In the design of the Maryland cyclotron it was attempted to obtain this kind of flexibility. The following section presents the main features of this design philosophy to illustrate what can be done in practice.

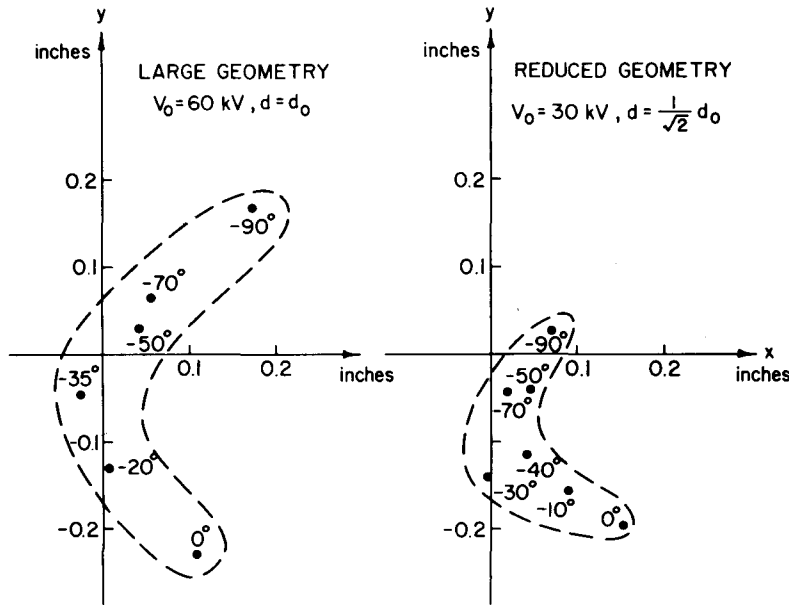


Fig. 4. Distribution of centre points for two scaled orbit geometries

### 3.2. Central-orbit design with variable duty factor in the Maryland cyclotron

The Maryland cyclotron, which features a four-sector magnetic field and  $90^\circ$  dees, has three modes of operation:  $N = \omega_{rf}/\omega = 1$ , push-pull;  $N = 2$ , push-push;  $N = 3$ , push-pull. The central region was designed for two main orbit geometries, one for the  $N = 1$  mode and one for the  $N = 2$  and  $N = 3$  modes. In each of these two fundamental geometries the dee voltage can be varied by as much as 50%, which permits a change of the orbit geometry by roughly 25%. The scaling radius  $R_o$ , which roughly corresponds to the orbit radius on the first half turn, is defined as:

$$R_o = \frac{1}{B} \left[ \frac{2m_o V_o \cos \theta_m}{q} \right]^{1/2} \quad (11)$$

where  $\theta_m$  is the phase angle of maximum energy gain; in our  $90^\circ$  dee system  $\cos \theta_m = 0.707$  for  $N = 1, 3$ , and  $\cos \theta_m = 1.0$  for  $N = 2$ . Table 1 gives the minimum and maximum values of  $R_o$  for each orbit geometry together with the number of turns. The highest voltage in each geometry is 60 kV and 90 kV respectively. Also given in Table 1 are the maximum turn separation  $\Delta r$  at extraction ( $r = 115$  cm), the source-puller spacing  $d$ , the initial phase width  $\Delta\theta_o$  of the acceptable beam and the width,  $\Delta\theta$ , after several turns which is smaller than  $\Delta\theta_o$  due to phase bunching.

The geometrical constraints of a  $90^\circ$ -dee system forbid the use of a single puller; we therefore use different pullers for each of the three modes of operation. Both ion source and puller can be adjusted to obtain the starting conditions for the various orbit geometries.

Fig. 5 shows the central region, equipotential lines (from electrolytic tank measurements) and initial orbits for protons with different starting phase in the  $N = 1$ , 60-kV geometry. The spatial position of the 'sausage' of ions at intervals of one-half rf period is marked; the intrinsic radial width of the ion sausage is depicted schematically. Energy gain and transit angle in the source-puller gap are plotted in Fig. 2 for both the 60-kV and 90-kV cases. It should be pointed out that the ion source was positioned such that a maximum of orbit centres would fall inside a circle with radius  $\Delta r_c = 0.1$  in. The figures for  $\Delta\theta_o$  and  $\Delta\theta$  in Table 1

**Table 1. ORBIT GEOMETRY PARAMETERS OF THE MARYLAND CYCLOTRON**

Parameter	N = 1		N = 2		N = 3	
	60 kV	90 kV	60 kV	90 kV	60 kV	90 kV
$\cos \theta_m$	0.707	0.707	1.000	1.000	0.707	0.707
$R_o$ (cm)	2.4	2.94	3.9	5.9	3.9	5.9
Turns $n$	680	450	230	155	230	155
$\Delta r_{extr.}$ (mm)	0.7	1.3	2.5	3.7	2.5	3.7
$d$ (mm)	9	16	9	16	9	16
$\Delta\theta_o$	55°	55°	70°	60°	40°	30°
$\Delta\theta$	40°	28°	30°	25°	15°	5°

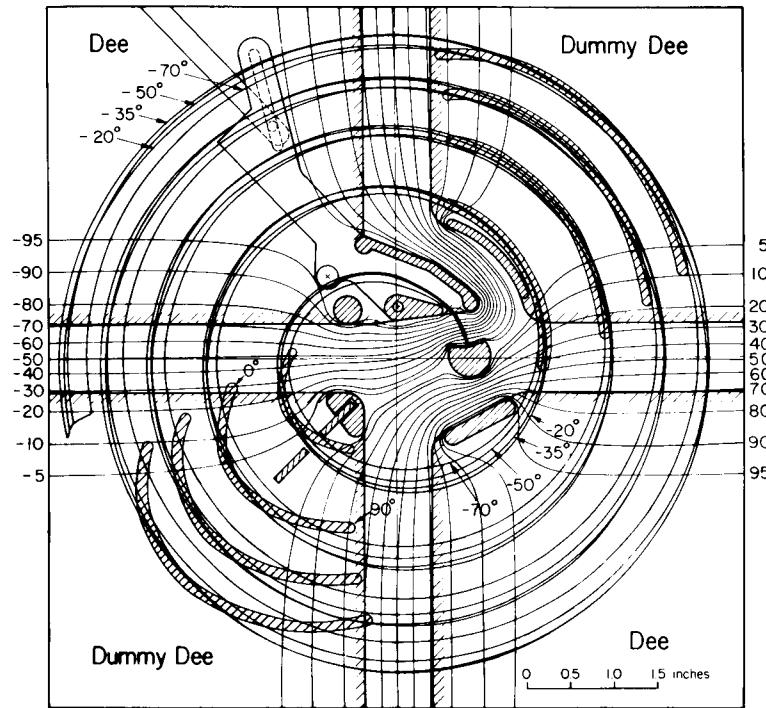


Fig. 5. Proton orbits for different starting phases in  $N = 1$ , 60-kV mode of Maryland cyclotron

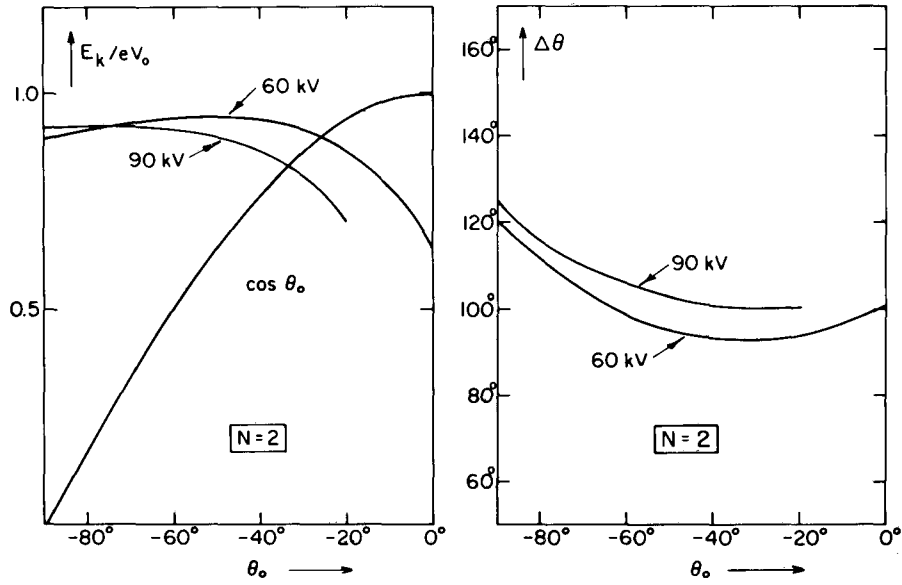


Fig. 6. Energy gain and transit phase angle in first gap for  $N = 2$ , 60 and 90 kV

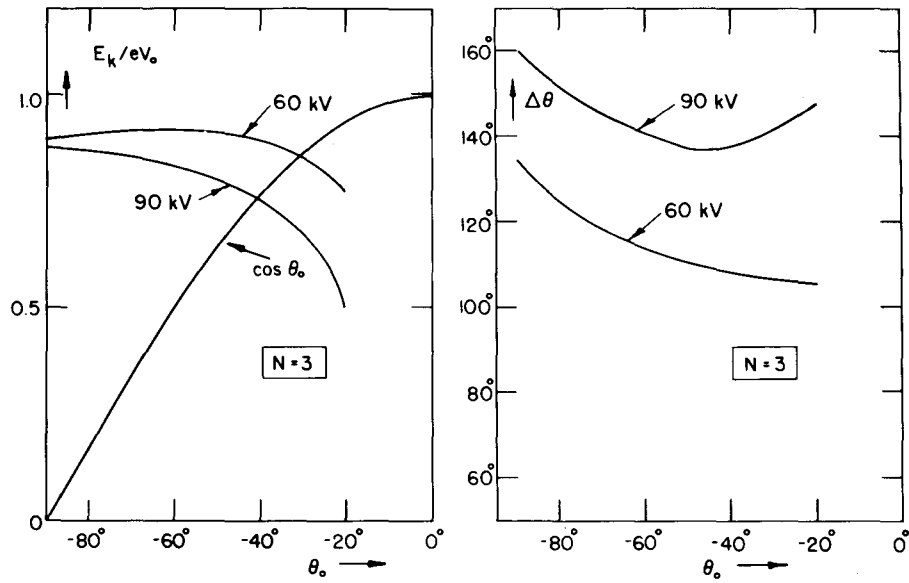


Fig. 7. Energy gain and transit phase angle in first gap for  $N = 3$ , 60 and 90 kV

300

represent the phase width for the group of ions whose centres were within the limit of 0.1 in.

Figs 6 and 7 show the energy gain and phase angle in the source-puller gap for the 60-kV and 90-kV geometries in the  $N = 2$  and  $N = 3$  modes. The phase width of the acceptable beam is listed in Table 1 for each case. One finds that  $\Delta\theta$  decreases when the dee voltage, and hence the orbit geometry, is increased in each mode. Of particular interest is the strong phase reduction which occurs when one changes from the  $N = 2$  to the  $N = 3$  mode. This is partly due to increased phase bunching in the third harmonic mode.

#### 4. SPACE-CHARGE EFFECTS AND VERTICAL FOCUSING

##### 4.1. Defocusing due to space charge

The current density, or the total beam current that can be successfully accelerated in a cyclotron is, as we know, limited by the repulsive Coulomb force due to the space charge of the ion bursts. The vertical electric field on the upper surface of the burst is approximately given by the equation:<sup>9</sup>

$$E_z = \frac{I}{\epsilon_0 \omega (\Delta\theta/2\pi) R_1^2} F(r) \quad (12)$$

The maximum current which can be transmitted through an area with vertical height  $z$  is:

$$I_{\text{lim}} = 2\epsilon_0 \frac{\Delta\theta}{2\pi} \omega z V_1 v_z^2 \frac{1}{F(r)}. \quad (13)$$

$V_1$  is the energy gain per turn and

$$R_1 = \frac{1}{B} \left[ \frac{2m_0 V_1}{q} \right]^{1/2}.$$

The factor  $F$  is a function of the turn number  $n$  or the radius  $r = R_1 \sqrt{n}$ . It has a maximum at the ion source decreasing roughly with  $1/r$  during the first turns and levelling off to a value of 1 at intermediate radii. A typical  $F(r)$  curve, taken from the author's paper on space charge effects,<sup>9</sup> is plotted in Fig. 8. If the vertical focusing frequency,  $\nu_z$ , is known, Eqn (13) permits an estimate of the maximum current that one can get through the available space inside the dee. (Blosser<sup>10</sup> made measurements of  $I_{\text{lim}}$  for the MSU cyclotron and found a relatively good agreement of 90% with the value predicted by the theory.) Perhaps more meaningful is to restrict the beam height to the 'linear' region close to the median plane (see Section 2.1) since most of the beam outside this region would either be difficult to extract or not be very useful to the experimenter due to the previously discussed phase-space distortions. (Actually most cyclotrons cannot handle the high currents of the space-charge limit, primarily due to cooling limitations in the extractor system.)

According to this theory one would like a  $\nu_z$  which increases as the radius gets smaller in order to balance the defocusing space-charge force which is

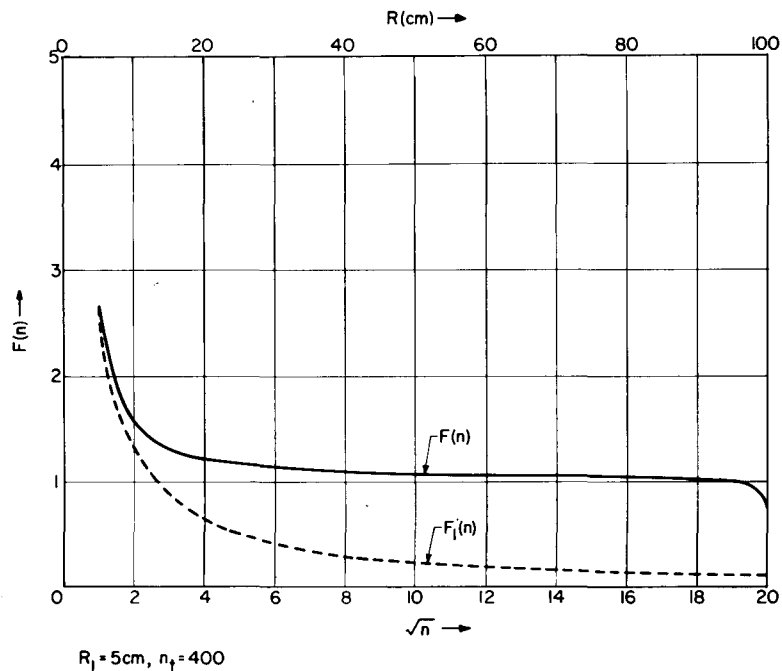


Fig. 8. Typical variation of relative space-charge force with radius

proportional to the function  $F(r)$ . Unfortunately, this is only the case for the equivalent  $\nu_{zel}$  of the electric focusing effect at positive phases. The more important focusing frequency due to the magnetic field goes to zero at  $r = 0$ . In the design of the Maryland cyclotron we attempted to get a  $\nu_z(r)$  curve in the centre which, although being far from ideal, takes the space-charge effects into account as is discussed in the following section.

#### 4.2. Gradient focusing in the centre of the Maryland cyclotron

The well-known disadvantage of a four-sector magnet structure is that the flutter and therefore  $\nu_z$  is weaker in the centre than in the case of a three-sector configuration. In the Maryland cyclotron  $\nu_z$  has a value of 0.2 at radii larger than 10 in, but decreases rapidly towards smaller radii due to the decreasing flutter. To fill this gap in the  $\nu_z(r)$  curve we decided to use a field bump in the centre producing additional gradient focusing. This bump was designed to (a) limit the phase shifts in each mode to acceptable values, and (b) give a peak in  $\nu_z$  close to the source position for optimum space-charge compensation. The  $\nu_z$  curve obtained under these conditions is plotted in Fig. 9 which also shows the average field,  $B(r)$ , the flutter amplitude (of the fourth harmonic in the field) and the equivalent  $\nu_z$  curves representing the electrical focusing effect for ions at  $0^\circ$ ,  $20^\circ$ , and  $40^\circ$  with respect to the rf voltage.

The bump in the magnetic field is produced with a cobalt-iron plug (diam.  $3\frac{1}{8}$  in) which can be adjusted in height over a range of 0.6 in thereby permitting a satisfactory optimisation of the  $\nu_z$  curve at all field levels.

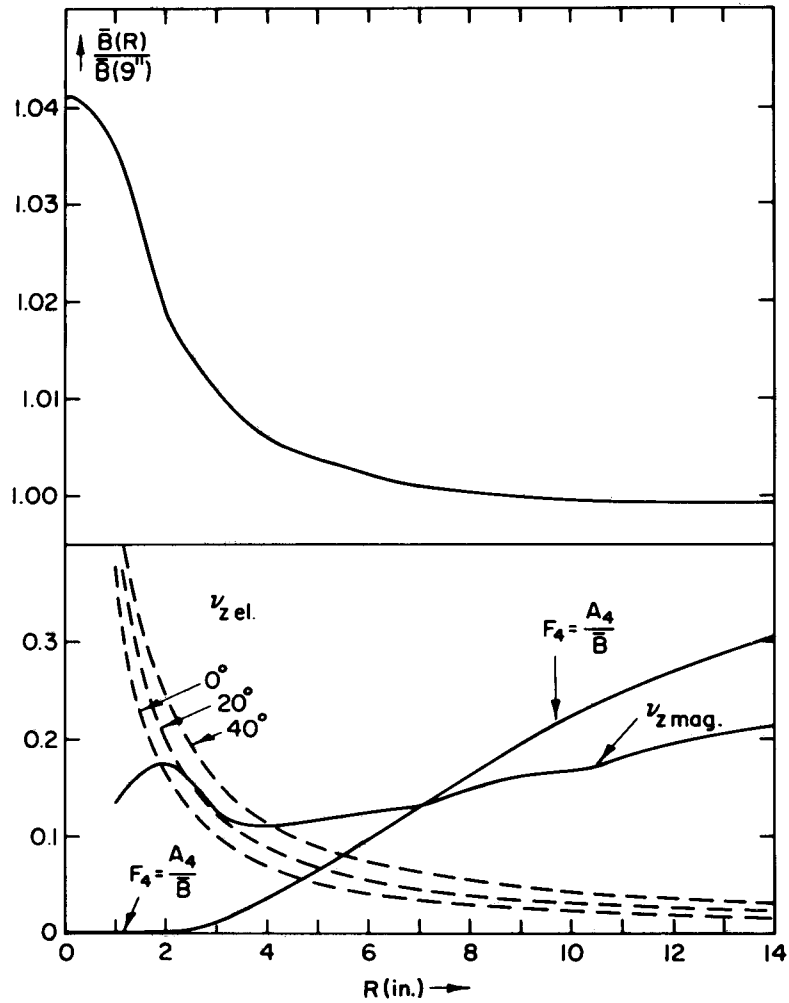


Fig. 9. Average field, flutter, electric and magnetic  $v_z$  vs radius in centre of Maryland cyclotron

#### 4.3. Electrical focusing

While the vertical magnetic force goes to zero as  $r$  decreases in the centre, the strength of the electric focussing or defocussing effects increase, reaching—like the space-charge force—a maximum at the ion source. By proper programming of the phase of the ions with respect to the rf (via off-setting the puller, etc.) one can place the useful group of ions into a focusing phase interval and thus close the gap due to the lack of adequate magnetic focusing on the early orbits. However, if one aims at a large duty-factor beam, overfocusing at the positive (lagging) end and defocusing at the negative (leading) end of the phase interval may lead to loss of beam. A careful study of vertical motion is therefore of great benefit and helps to define and optimise the width of the 'transmission window' in the rf period. In the past such investigations were hampered by the fact that the

analytic theory<sup>11</sup> by Rose and Cohen is not valid in the neighbourhood of the ion source and field mapping in this region was restricted to median-plane potential distributions (electrolytic tank) or simulated vertical fields.<sup>12</sup> In contrast to magnetic field measurement, where  $B_z$  is obtained directly, electrolytic-tank data of the median-plane potential distribution is not accurate enough to permit expansion in  $z$  and calculation of the  $z$  component of the electric field.

We have over the past years at the University of Maryland done extensive studies of the electric focusing problem. The scope of this paper excludes a detailed discussion of this work, but the main points shall be briefly mentioned. We have basically worked in two directions. One was the extension of the Rose-Cohen theory to include the effects of the dee liner.<sup>13</sup> It was found that the presence of the liner above the acceleration gap reduces the strength of the

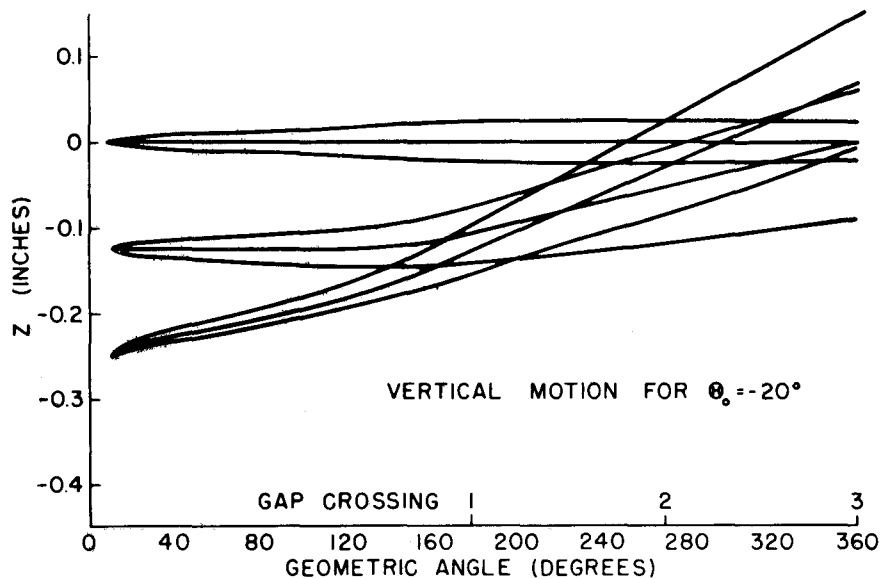


Fig. 10. Calculated vertical motion of particles on first turn in Maryland cyclotron

electrostatic focusing effect by a factor which depends on the gap width, internal dee height, and the dee-to-liner spacing. The second major effort was an extension of the electrolytic-tank method to measure potentials off the median plane (i.e. below the surface of the electrolyte).<sup>14</sup> By proper probe design, choice of suitable current densities in the electrolyte and other measures it was possible to get accuracies of a few tenths of a per cent, comparable to the accuracies obtained in the median plane (surface of the electrolyte). By this technique potential distributions near the ion source of the Maryland cyclotron were mapped. The data was taken in the median plane and five planes off the median plane. A computer code called TRIWHEEL was developed and three-dimensional ion motion was calculated. Fig. 10 shows some results of these calculations. It presents the vertical motion of a group of protons ( $N = 1$ , 60 kV case) leaving the ion source. Nonlinear effects are clearly discernable. In addition

to this electrolytic-tank work we have developed a computer program which permits potential mapping by the relaxation method.<sup>15</sup> While the electrolytic tank gives better results close to the ion source, the relaxation method is superior in the region outside the first orbit. Vertical motion studies with TRIWHEEL, calculating the orbits over several turns, proved that most of the large duty factor beam is well focused and losses due to over-focusing or defocusing should be small in this mode of cyclotron operation.

#### ACKNOWLEDGEMENTS

I wish to thank Dr. Hogil Kim for many valuable discussions concerning duty factor and beam quality. Some of the studies reported in this paper were carried out with the assistance of Dr. F. Dupont (CSF), Mr. C. Han, and Mr. T. Zinneman whose contributions are gratefully acknowledged.

#### DISCUSSION

Additional remarks by M. Reiser (Maryland).

I wish to make a brief comment on the status of the Maryland cyclotron. We have successfully accelerated  $10\ \mu\text{A}$  of  $\alpha$ -particles to 60 MeV using calculated trim coil settings based on the field maps. Except for some loss of beam at small radii there was practically no attenuation from 10 in to the full radius of 45 in. In preliminary trial runs a few per cent of this beam was also extracted through the electrostatic and magnetic channels. In the next few months it is planned to do further work on the rf system and cope with the usual instrumentation and calibration problems that occur at this stage of such a project. After that we intend to go into a systematic beam development programme and start doing nuclear experiments.

#### REFERENCES

1. Blosser, H. G., *I.E.E.E. Trans.* NS-13, 1, (1966).
2. Leboutet, H., *I.E.E.E. Trans.* NS-14, 881, (1967); Johnson, T. H., *et al. I.E.E.E. Trans.* NS-16, 438, (1969).
3. Reiser, M., *et al. I.E.E.E. Trans.* NS-16, 448, (1969).
4. Mallory, M. L. and Reiser, M., *I.E.E.E. Trans.* NS-12, 817, (1965); Mallory, M. L. and Blosser, H. G., *I.E.E.E. Trans.* NS-13, 163, (1966).
5. Reiser, M., MSU Cyclotron Report No. 16, March 1963; Proc. of 1963 Cyclotron Conf., CERN 63-19, 195, (1963).
6. Reiser, M., *Nucl. Instr. Meth.* 18, 19, 370, (1962).
7. Lawson, J. D., *I.E.E.E. Trans.* NS-14, 635, (1967).
8. Reiser, M., CERN 63-19, 203, (1963).
9. Reiser, M., *I.E.E.E. Trans.* NS-13, 171, (1966).
10. Blosser, H. G., private communication.
11. Rose, M. E., *Phys. Rev.* 53, 392, (1938); Cohen, B. L., *Rev. Sci. Instr.* 24, 589, (1953).
12. Blosser, H. G. and Gordon, M. M., CERN 63-19, 197, (1963).
13. To be published.
14. Zinneman, T. E., Three-Dimensional Electrolytic Tank Measurements and Vertical Motion Studies, Report No. 986, June 1969, Dept. of Physics and Astronomy, University of Maryland.
15. Nelson, D., *et al. I.E.E.E. Trans.* NS-16, 766, (1969).